Journal Club - IBM Research Zurich - University of Basel

High fidelity state preparation, quantum control, and readout of an isotopically enriched silicon spin qubit

Authors: A. R. Mills, C. R. Guinn, M. M. Feldman, A. J. Sigillito, M. J. Gullans, M. Rakher, J. Kerckhoff, C. A. C. Jackson, and J. R. Petta

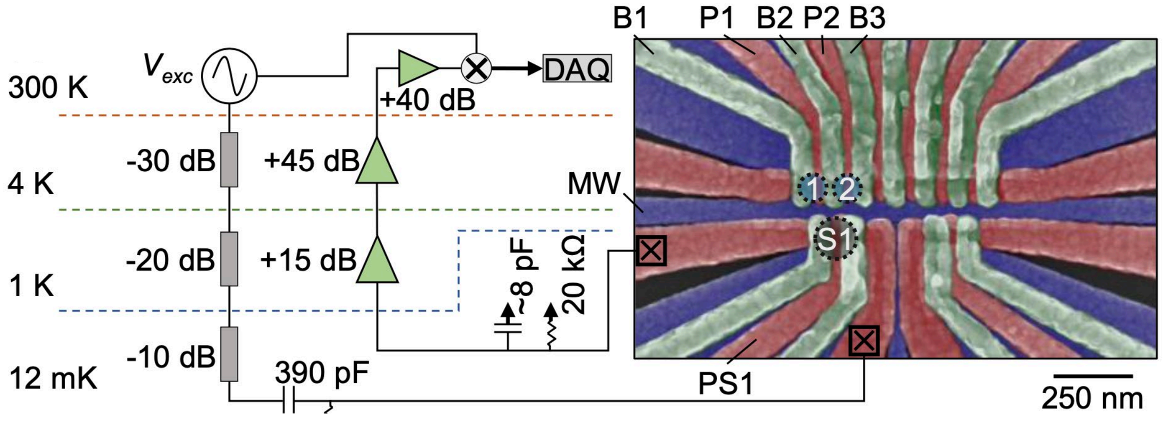

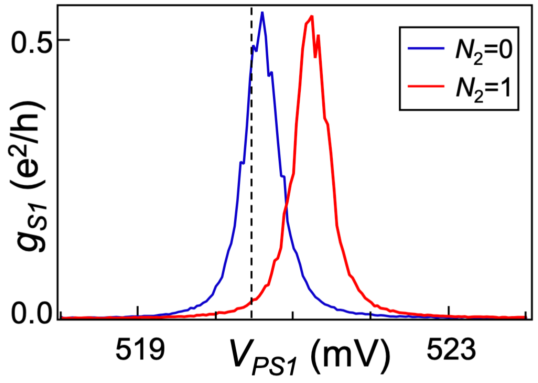

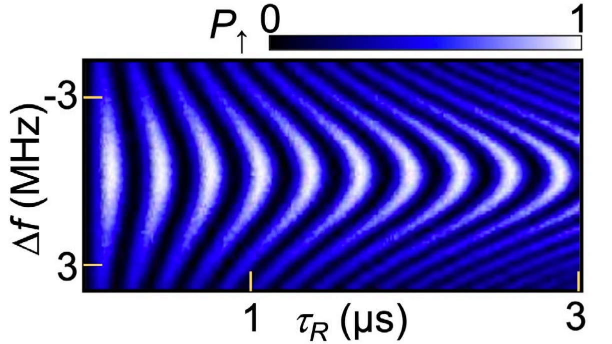

Leonardo Massai - LEM

30.05.2022

Summary

1. Introduction
   - Requirements for 99% visibility

2. System overview and optimizing oparation parameters
   - Measurement circuit for readout
   - Charge sensor and spin-to-charge conversion
   - Data acquisition parameters

3. SPAM and Single Qubit Gates fidelities
   - GST and IRB fidelities

4. Conclusions

Requirements for 99% visibility

- For a LD spin qubit that uses Elzerman readout, the minimum requirements for achieving 99% visibility are [1]:

1. large Zeeman splitting E_z relative to the electron temperature T_e, $E_z \gtrsim 13 k_B T_e$
2. fast tunnel out time $t_{out}^{\uparrow}$ for a spin-up electron relative to the spin relaxation time T_1, $T_1 \gtrsim 100 t_{\uparrow out}$
3. fast sampling rate Γ_s relative to the reload rate $1/t_{in}^{\downarrow}$, $\Gamma_s \gtrsim 12/t_{in}^{\downarrow}$.

If any of these requirements are not met, 99% visibility Elzerman spin readout is not possible.

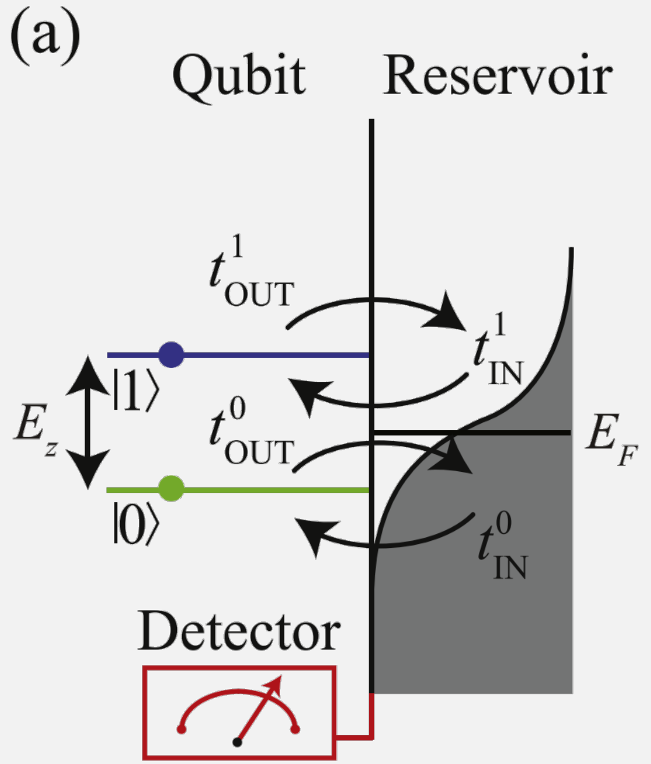

[1] D. Keith, S. K. Gorman, L. Kranz, Y. He, J. G. Keizer, M. A. Broome, and M. Y. Simmons, Benchmarking high fidelity single-shot readout of semiconductor qubits, New J. Phys. 21, 063011 (2019).

Summary

1. Introduction
   - Requirements for 99% visibility
2. System overview and optimizing oparation parameters
   - Measurement circuit for readout
   - Charge sensor and spin-to-charge conversion
   - Data acquisition parameters
3. SPAM and Single Qubit Gates fidelities
   - GST and IRB fidelities
4. Conclusions

Device

- The device [0]:
  - Si/SiGe heterostructure with an isotopically purified ^{28}Si (800 ppm residual ^{29}Si) quantum well
  - Lithographically defined overlapping aluminum gate electrodes
  - 6 quantum dots with 2 proximal charge sensors

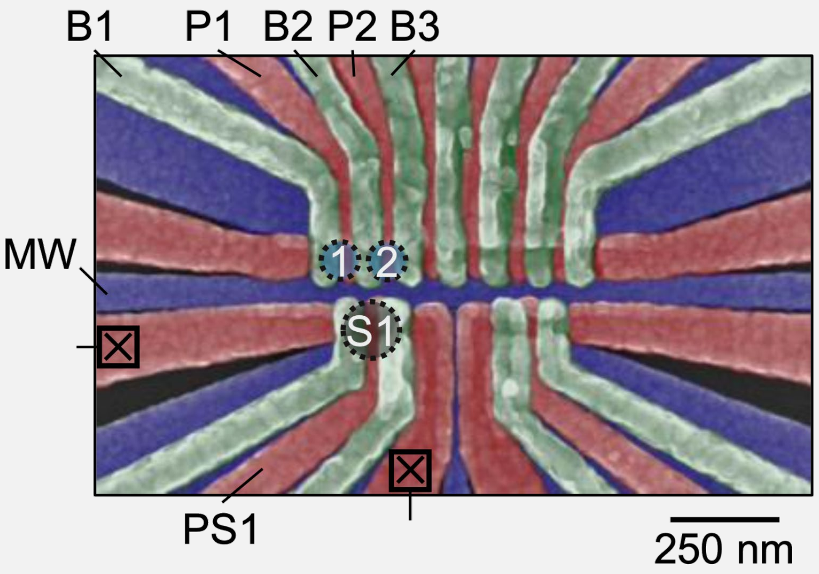

[0] D. M. Zajac, T. M. Hazard, X. Mi, K. Wang, and J. R. Petta, A reconfigurable gate architecture for Si/SiGe quantum dots, Appl. Phys. Lett. 106, 223507 (2015)

Measurement circuit for readout

- Optimization of charge state readout:
  - V_{exc} @ 1 MHz is applied to S1 and the drain current flows to ground through a 20 kΩ resistor
  - The voltage drop across the 20 kΩ resistor is amplified by 2 high-electron mobility transistors (HEMT) @ 1K and 4K before a RT amplifier
  - c_p~8 pF which limits the circuit bandwidth to ~1 MHz

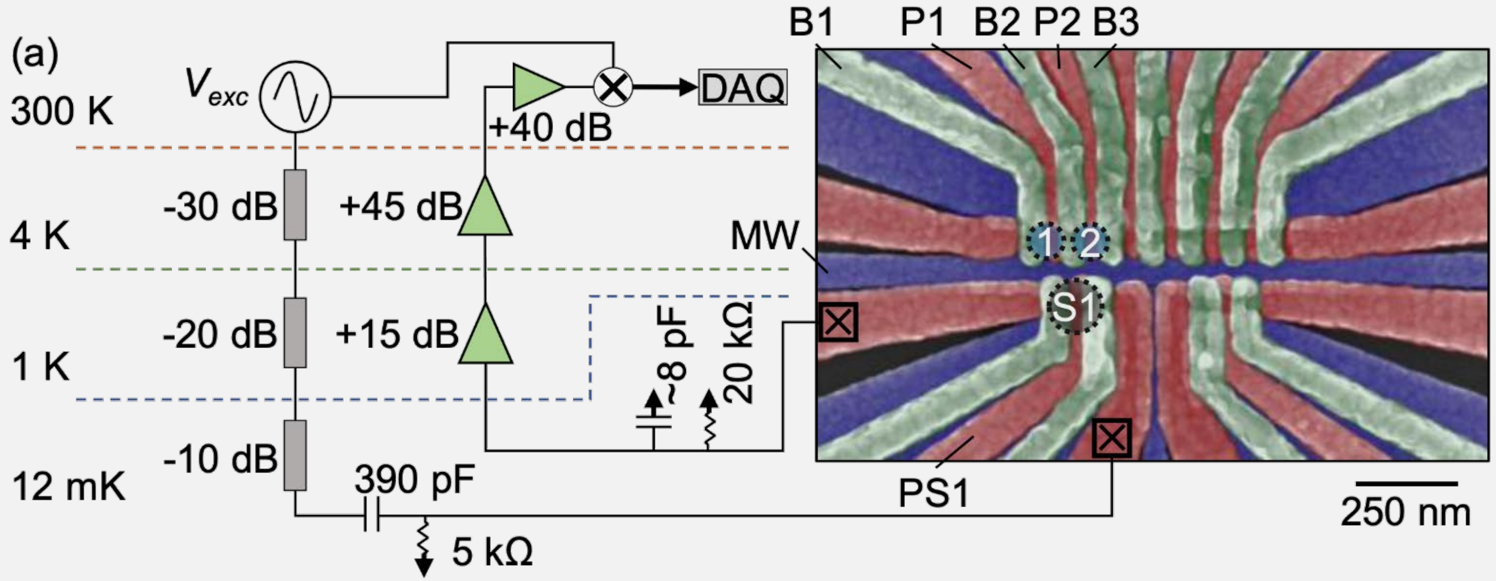

Charge sensor – Coulomb blockade

- Coulomb blockade peak in the charge sensor conductance g_{S1} as the sensor dot plunger gate voltage V_{PS1} is swept
- Changing $N_2 = 0$ to $N_2 = 1$ shifts the Coulomb blockade peak by $\sim$ its FWHM
- When biased on the side of a Coulomb blockade peak the sensor dot can easily detect real-time tunneling events

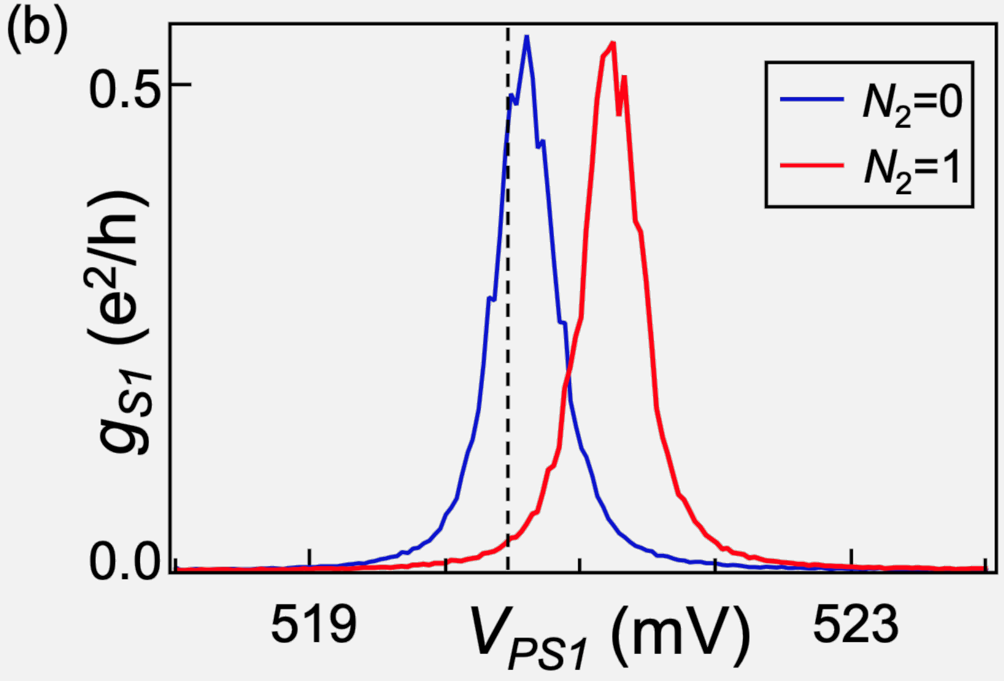

Charge sensor – Coulomb blockade

- Real-time g_{S1} sampled at $1\ \mathrm{MS/s}$ with chemical potential $\mu_2 \sim E_{F,Res}$
- The switching rate between $N_2 = 0$ and $N_2 = 1$ is set by the tunnel coupling Γ between the D_2 and Res. to be slower than measurement bandwidth
- The charge readout SNR is set by the separation of the two Gaussians relative to their spread: $SNR = (m_0 - m_1)/\bar{\sigma}$ with $\bar{\sigma} = (\sigma_1 + \sigma_0)/2$

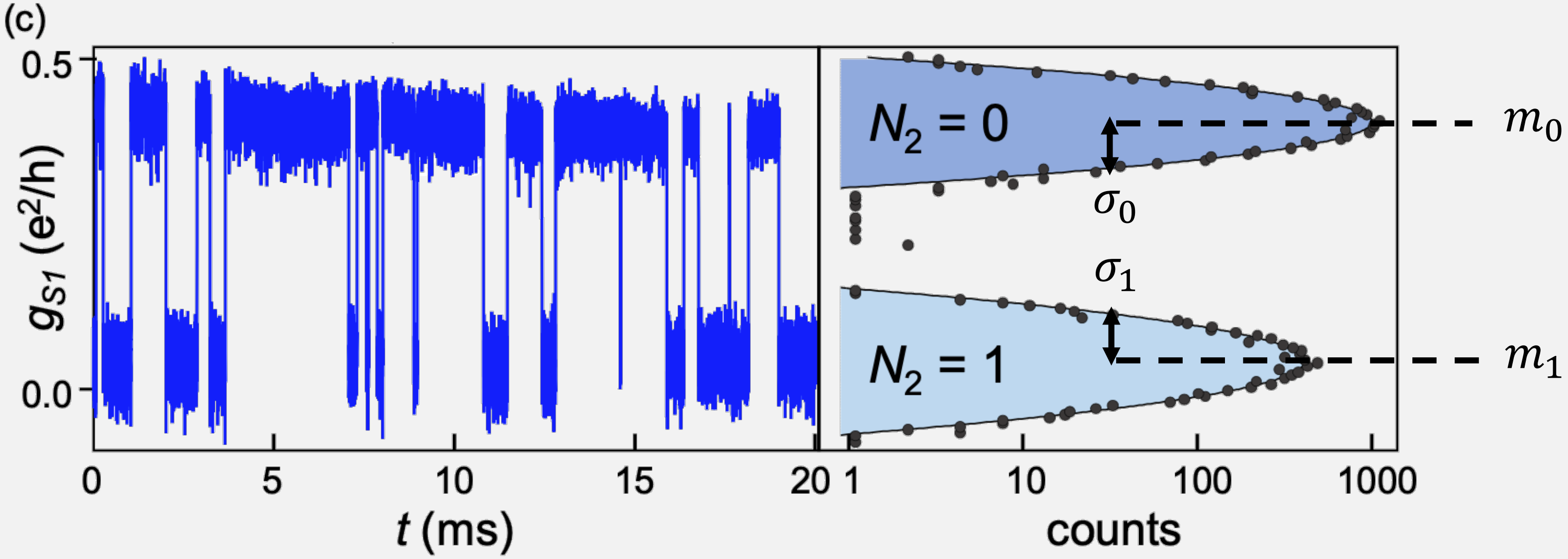

Charge sensor – SNR and T_e

❖ SNR and electron temperature T_e as a function of the peak-to-peak excitation voltage V_{exc} from the charge sensor.

- Operation voltage: $V_{exc} = 85\ \mu\mathrm{V_{pp}}$, where the $SNR \approx 12.5$ and $T_e \approx 45\ \mathrm{mK}$.
- The electron temperature is estimated by the broadening of the tunneling line width for the first electron dot-reservoir transition.
- Values of $T_e \ll 200\ \mathrm{mK}$ [2,3].

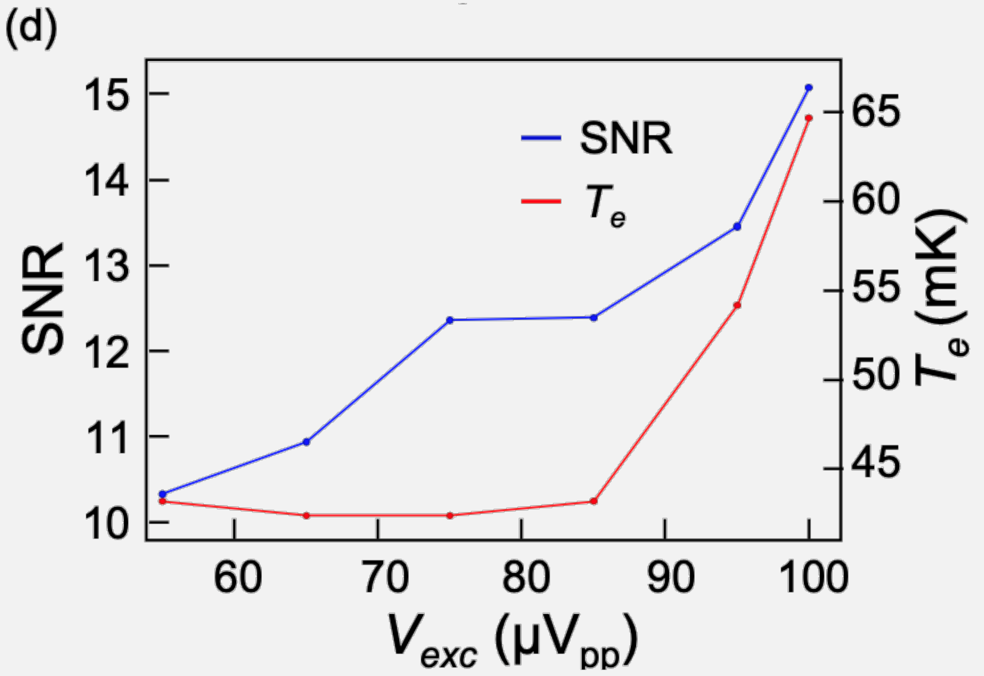

[2] D. Keith et al, Single-shot spin readout in semiconductors near the shot-noise sensitivity limit, Phys. Rev. X 9, 041003 (2019).

[3] A. Morello et al, Single-shot read- out of an electron spin in silicon, Nature (London) 467, 687 (2010).

Charge sensor – SNR and T_e

❖ SNR and electron temperature T_e as a function of the peak-to-peak excitation voltage V_{exc} from the charge sensor.

- In theory a $SNR = 12.5$ yields a lower bound estimate of the charge state infidelity $1 - F_c \geq 3e^{-10}$ [4].

- The negligible charge state infidelity implies that the overall readout performance will be limited by the spin-to-charge conversion process.

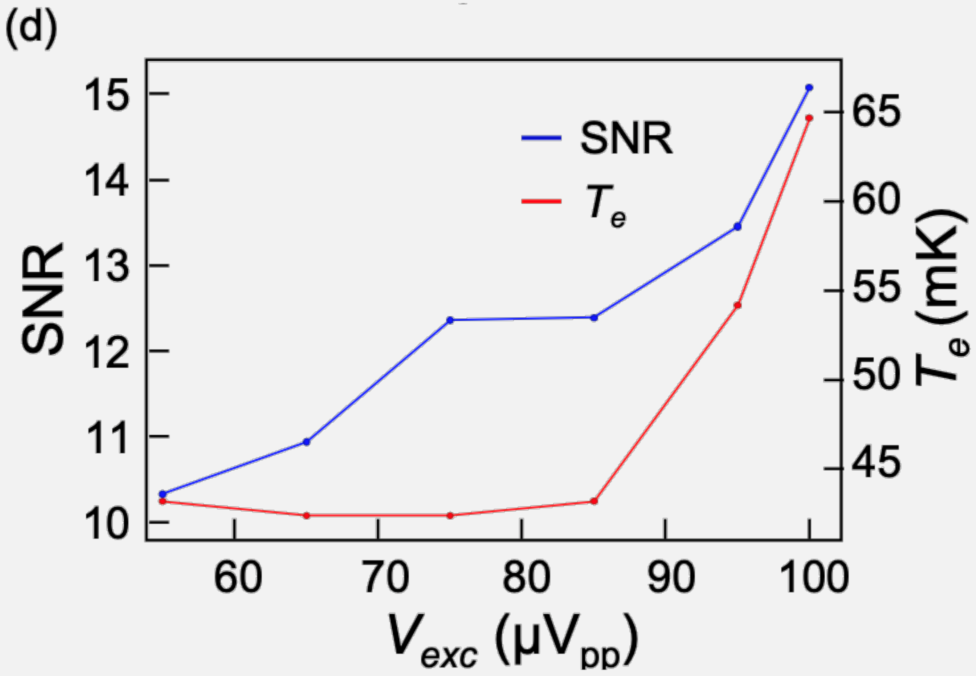

[4] J. Z. Blumoff et al., Fast and high-fidelity state preparation and measurement in triple-quantum-dot spin qubits, arXiv:2112.09801 (2021).

Spin-to-charge conversion

❖ Process of spin-to-charge conversion for a spin-up electron:

- The $|\uparrow\rangle$ e- tunnels off the dot in $\sim 1/\Gamma_{out}^{\uparrow}$ and is replaced by $|\downarrow\rangle$ e- that tunnels into the dot in $\sim 1/\Gamma_{in}^{\downarrow}$.

- $1/\Gamma_{out}^{\uparrow} < T_1$ and $\Gamma_{in}^{\downarrow}$ must be slow enough to be detectable, given the finite bandwidth of the measurement circuit

- The overall tunnel rate Γ is set by V_{B3}
- $\Gamma_{out}^{\uparrow}/\Gamma_{in}^{\downarrow}$ is adjusted by Δ $(E_{F,Res} - E_{|\downarrow\rangle})$

- $B_{ext} = 410\ \mathrm{mT}$, with $E_Z = 19.105\ \mathrm{GHz}\ (79\ \mu\mathrm{eV})$ and $T_1 = 31.5\ \mathrm{ms}$

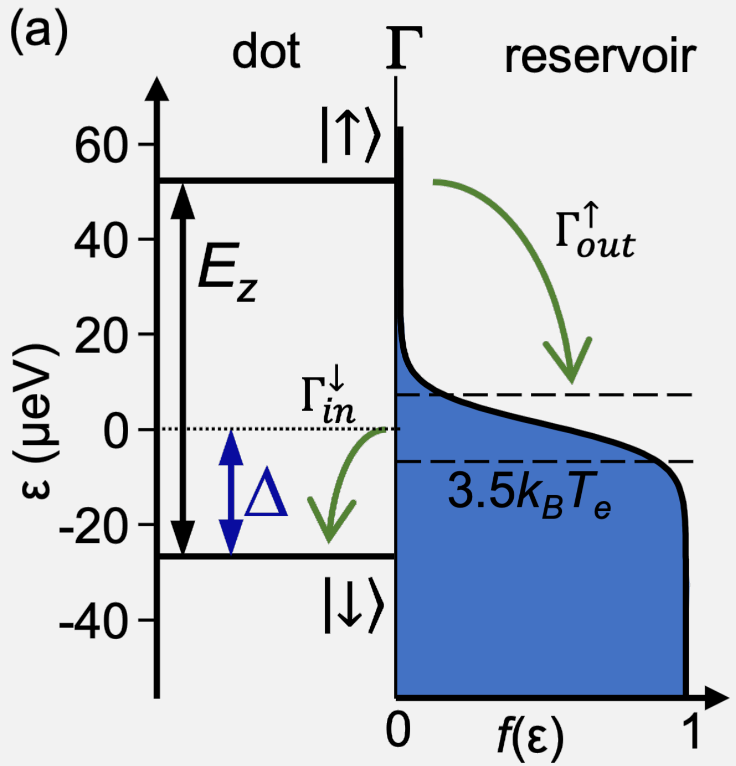

Spin-to-charge conversion

❖ Process of spin-to-charge conversion for a spin-up electron:

- The optimal Δ is large enough to suppress thermal errors and small enough to maximize the ratio $\Gamma_{out}^{\uparrow}/\Gamma_{in}^{\downarrow}$

- The rates $\Gamma_{out}^{\uparrow}$ and $\Gamma_{in}^{\downarrow}$ are extracted by the tunneling times from many single shot traces Fig. (b) and fitting to an exponential decay

- Fig. (c) shows the visibility $V = F_{\uparrow} + F_{\downarrow} - 1$ (preparing 10000 states and measuring) in function of Δ

- The optimal values: $\Delta^{*} \approx 30\ \mu\mathrm{eV}$ resulting in $\Gamma_{out}^{\uparrow} \approx \Gamma_{in}^{\downarrow} \approx 20\ \mathrm{kHz}$

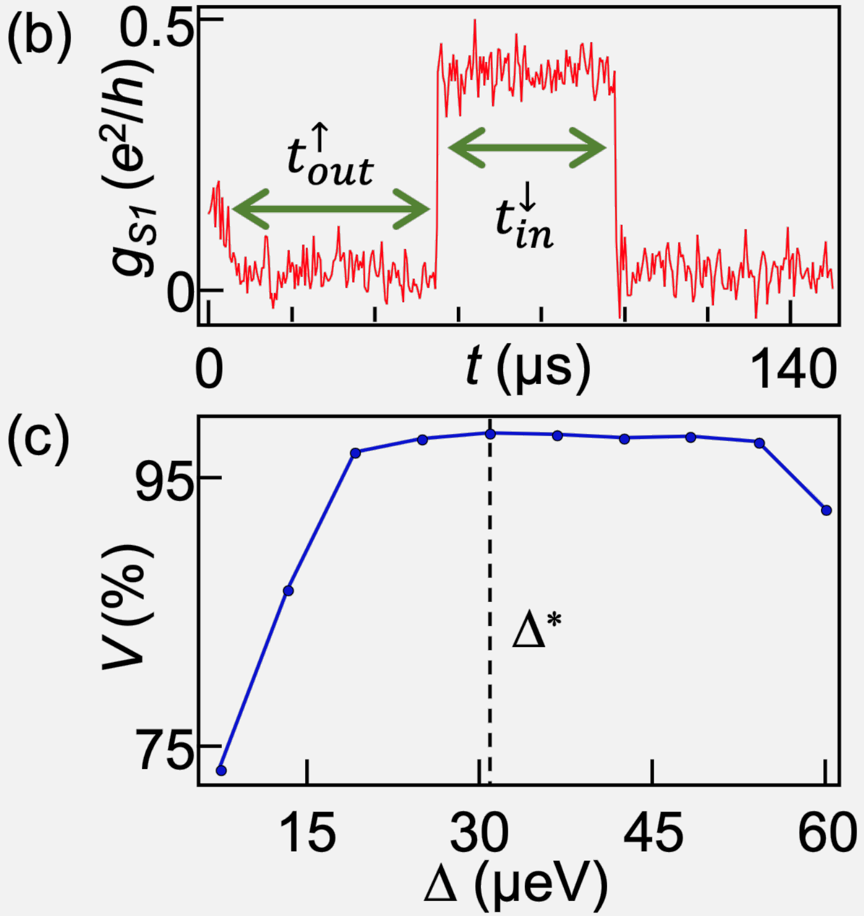

Data acquisition parameters

❖ Optimization of data acquisition parameters:

- Conductance threshold g_{thr} and duration of the readout window t_R

- $|\uparrow\rangle$ state is registered when $g_{S1} > g_{thr}$ within the time window t_R, Fig. (a)

- If g_{thr} is set too low ⇒ noise can lead to false positives ($F_\downarrow$ ↘)
- If g_{thr} is set too high ⇒ we miss the short events that don't reach full amplitude ($F_\uparrow$ ↘)

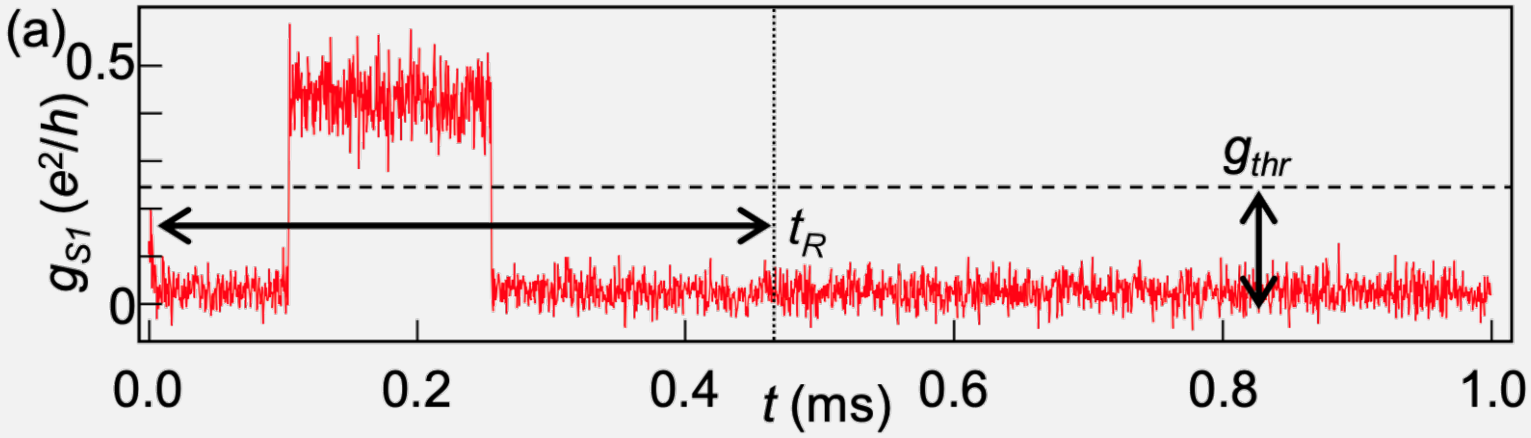

Data acquisition parameters

❖ Optimization of data acquisition parameters:

- Conductance threshold g_{thr} and duration of the readout window t_R

- if t_R is too low ⇒ not able to catch all hopping events from spin-to-charge conversion ($F_\uparrow$ ↘)
- if $t_R \gg t_{out}^{\uparrow}$ ⇒ more thermal errors ($F_\downarrow$ ↘)

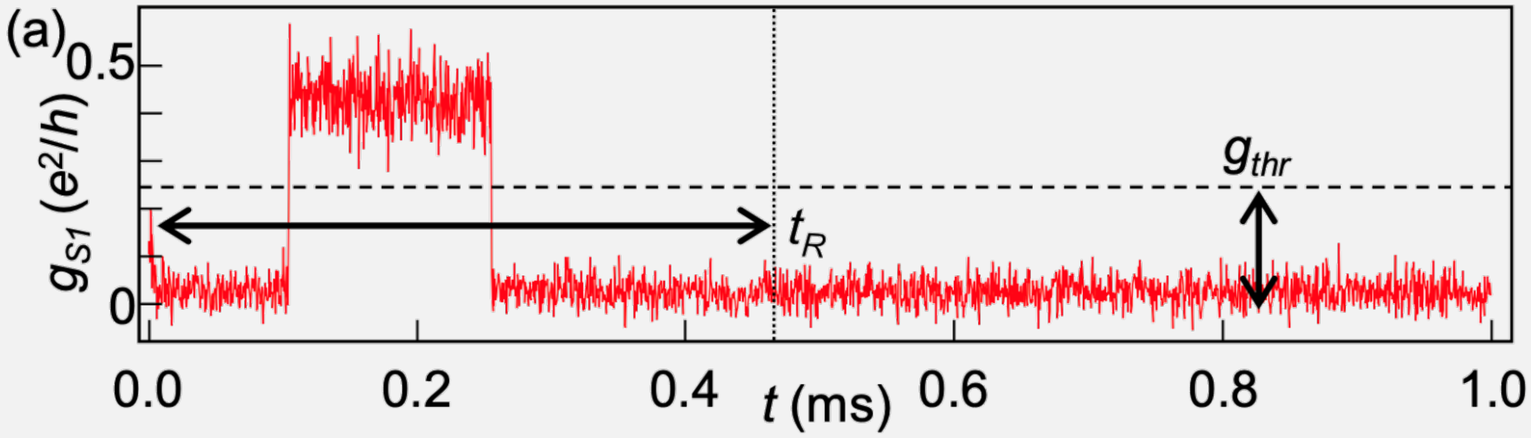

Data acquisition parameters

❖ Optimization of data acquisition parameters:

- Conductance threshold g_{thr} and duration of the readout window t_R
- Optimization of g_{thr} and t_R preparing 10000 states and measuring, using the optimized Δ^*
- Fidelity F as a function of g_{thr}:
  $\Rightarrow$ Optimal $g^*_{thr} = 0.22\ \mathrm{e}^2/\mathrm{h}$, Fig. (b)

  - If $g_{thr} \searrow \quad \Rightarrow F_{\downarrow} \searrow$
  - If $g_{thr} \nearrow \quad \Rightarrow F_{\uparrow} \searrow$

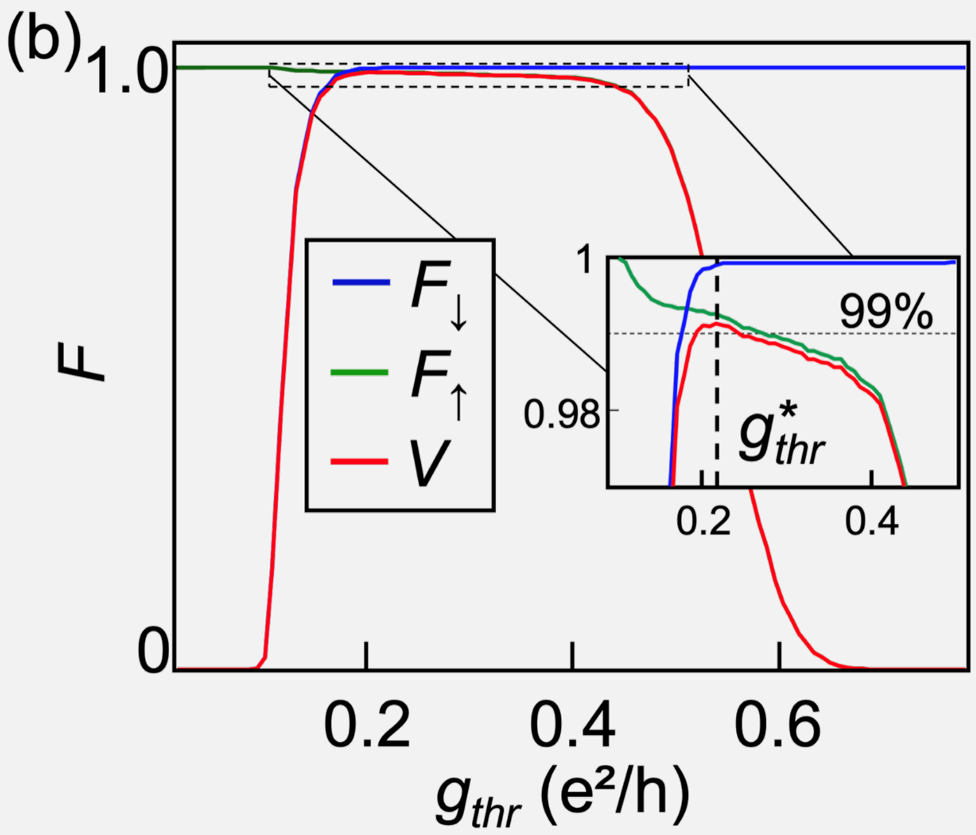

Data acquisition parameters

❖ Optimization of data acquisition parameters:
- Conductance threshold g_{thr} and duration of the readout window t_R
- Optimization of g_{thr} and t_R preparing 10000 states and measuring, using the optimized Δ^*
- Measurement infidelities $1 - F$ as a function of t_R:

  $\Rightarrow$ Optimal $t_R^* = 670\ \mu s$, Fig. (c)

  - If $t_R \searrow \quad \Rightarrow F_\uparrow \searrow$
  - If $t_R \nearrow \quad \Rightarrow F_\downarrow \searrow$

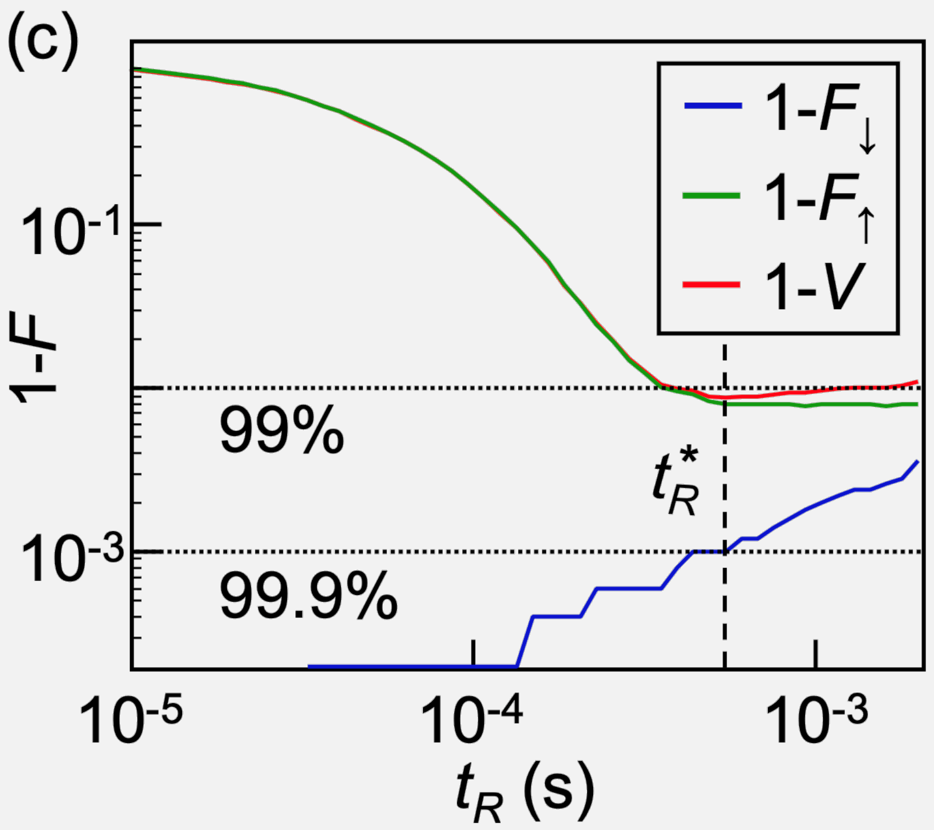

Summary

1. Introduction
   - Requirements for 99% visibility

2. System overview and optimizing oparation parameters
   - Measurement circuit for readout
   - Charge sensor and spin-to-charge conversion
   - Data acquisition parameters

3. SPAM and Single Qubit Gates fidelities
   - GST and IRB fidelities

4. Conclusions

Fidelities with optimized parameters

- Reached fidelities with optimized parameters (V_{PS1}^*, V_{exc}^*, Δ^*, g_{thr}^* and t_R^*):

  - $F_\downarrow = 99.86\% \pm 0.05\%$, $F_\uparrow = 99.26\% \pm 0.12\%$
    $\Rightarrow$ average measurement fidelity $F_M = 99.56\%$

  - The probability of missing a spin bump
    $P_{miss} = 1 - \frac{\left(1-e^{(R_S^\uparrow - R_S^\downarrow)/2}\right)R_S}{\left(1-e^{R_S^\uparrow/2}\right)\left(R_S^\uparrow - R_S^\downarrow\right)}$ with $R_S^\uparrow = t_S/t_{out}^\uparrow$, $R_S^\downarrow = t_S/t_{in}^\downarrow$ *and* $t_S = 1$ µs (sampling rate)

Rabi oscillations

❖ Rabi oscillations

- Spin-up probability $P_\uparrow$ as a function of the frequency detuning Δf from resonance $(19.105\ \mathrm{GHz})$ and the microwave burst length τ_R, Fig. (a).

- Rabi oscillations at resonance, Fig. (b).

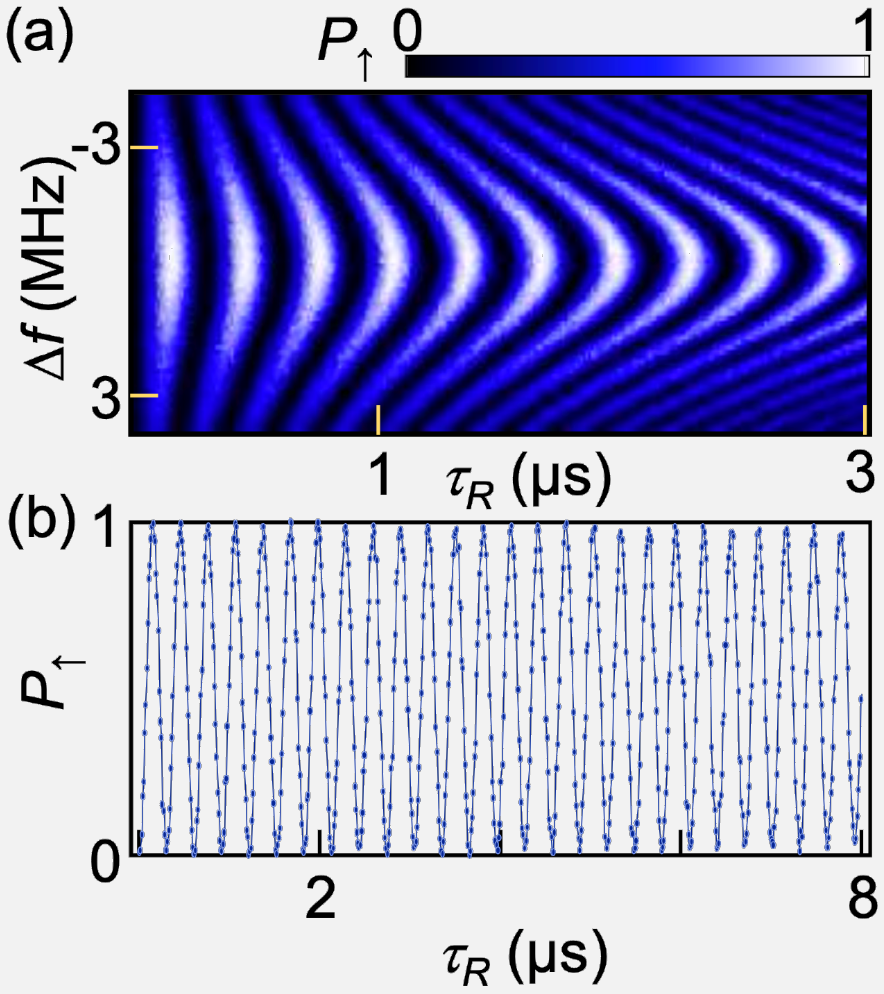

Gate and SPAM fidelities - GST

- Gate and State Preparation And Measurement (SPAM) fidelities

  - High gate and SPAM fidelities verified using Gate Set Tomography (GST) protocols for single qubit gates (I, X, Y) [5]

  - GST yields to:
    - $\rho_{0,GST} = 99.76\% \pm 0.04\%$
    - $M_{GST} = 99.35\% \pm 0.1\%$
    - $\mathrm{SQG}_{\mathrm{GST}} = 99.956\% \pm 0.002\%$

  - The gate fidelity is limited by incoherent noise ($T_2^* = 3.2$ µs, $T_2^H = 139$ µs measured using Ramsey and Hahn echo pulse sequences)

[5] E. Nielsen, J. K. Gamble, K. Rudinger, T. Scholten, K. Young, and R. Blume-Kohout, Gate Set Tomography, Quantum 5, 557 (2021).

Gate and SPAM fidelities - IRB

❖ $(X, X^2, -X, Y, Y^2, -Y)$ fidelities with Interleaved Randomized Benchmarking (IRB) [6]:

- $k = 200$ unique sequences per point, with 100 averages
- Sequence lengths of up to $N_{C1} = 4096$ Clifford operations are employed to achieve full saturation of the sequence fidelity curves, Fig. (c).

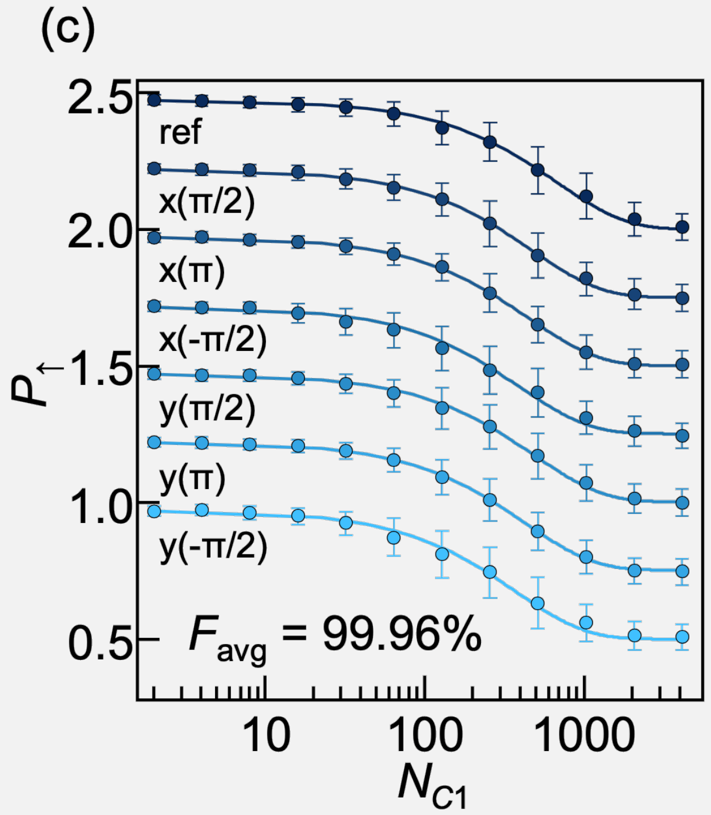

- traces shifted by 0.25

[6] E. Magesan, J. M. Gambetta, and J. Emerson, Scalable and robust randomized benchmarking of quantum pro- cesses, Phys. Rev. Lett. 106, 180504 (2011).

Gate and SPAM fidelities – GST & IRB

- Average gate fidelities, Table 1:
  - Retuning routines every ~ 30 mins during long measurements (~ 14 hrs.) to correct for readout and qubit frequency drifts
  - The charge sensor excitation is turned off during qubit manipulation to reduce heating at the device

IRB Fidelities		GST Fidelities	
Gate	Fidelity	Operation	Fidelity
X	99.969% ±0.004%	ρ_0	99.76% ±0.04%
X^2	99.964% ±0.003%	M	99.35% ±0.1%
$-X$	99.949% ±0.005%	I	99.43% ±0.036%
Y	99.973% ±0.004%	X	99.958% ±0.002%
Y^2	99.961% ±0.004%	Y	99.954% ±0.002%
$-Y$	99.937% ±0.005%		

Summary

1. Introduction
   - Requirements for 99% visibility

2. System overview and optimizing oparation parameters
   - Measurement circuit for readout
   - Charge sensor and spin-to-charge conversion
   - Data acquisition parameters

3. SPAM and Single Qubit Gates fidelities
   - GST and IRB fidelities

4. Conclusions

Conclusions

❖ Si spin qubits can be operated reliably with all-around high performance metrics:

- Optimal SPAM requires careful tuning of operation parameters to minimize the loss of spin information due to relaxation and a finite $1\ \mathrm{MHz}$ measurement bandwidth

- Measurement fidelities $> 99\%$

- GST and IRB are implemented to demonstrate average SQG fidelities $> 99.95\%$ under the same operating conditions